photonics

MDPI

Communication

Synchronization of Optomechanical Oscillators in Coupled 1D Optomechanical Crystal Nanobeam Cavities

Yang Liu [1,2,3], Fei Gao [4], Daquan Yang [5], Aiqiang Wang [1,2,*], Mengchen Zhou [1,2], Shanchuang Li [1,2], Lu Gao [6] and Ze Zhang [1,2]

1 Qilu Aerospace Information Research Institute, Jinan 250100, China
2 Aerospace Information Research Institute, Chinese Academy of Sciences, Beijing 100094, China
3 Science and Technology on Solid-State Laser Laboratory, Beijing 100015, China
4 Department of Physics & Astronomy, Rice University, Houston, TX 77005, USA
5 School of Information and Communication Engineering, Beijing University of Posts and Telecommunications, Beijing 100876, China
6 School of Science, China University of Geosciences, Beijing 100083, China
* Correspondence: wangaq01@aircas.ac.cn

Abstract: We proposed a new optomechanical system (OMS) based on parallel suspended one-dimensional optomechanical crystal (1D-OMC) nanobeam cavities for optomechanical synchronization. The optomechanical oscillators (OMOs) were spaced apart by an air-slot gap and coupled through optical radiation fields. The numerical simulation showed that the evolution process of 1D-OMC nanobeam cavities to mechanical synchronization could be divided into three clear stages. The synchronization of two mechanical breathing modes at 5.8846 GHz was achieved by using a single laser source. Finally, we investigated the relationship between the threshold power and detuning of an input laser for self-sustaining and synchronization states. Such chip-based structures hold great potential for large-scale synchronized oscillator networks.

Keywords: optomechanical synchronization; optomechanical crystal; optomechanical oscillators

Citation: Liu, Y.; Gao, F.; Yang, D.; Wang, A.; Zhou, M.; Li, S.; Gao, L.; Zhang, Z. Synchronization of Optomechanical Oscillators in Coupled 1D Optomechanical Crystal Nanobeam Cavities. *Photonics* **2022**, *9*, 743. https://doi.org/10.3390/photonics9100743

Received: 23 September 2022
Accepted: 6 October 2022
Published: 9 October 2022

1. Introduction

Synchronization has been widely observed in a large variety of fields, which is useful in applications of time-keeping [1], microwave communication [2], as well as in novel computing and memory [3,4]. Based on the development of nanofabrication technology, synchronized mechanical oscillators have been experimentally demonstrated in nanomechanical systems [5] and nanoelectromechanical systems with electronic coupling or physical connections [6,7]. Recently, optomechanical systems have emerged as an ideal platform for synchronization with high-quality resonance and strong optomechanical coupling [8–12].

The interaction between mechanical oscillators through light in OMS have good controllability and scalability. An example of such a system includes the synchronization of two optically coupled OMOs with small spacing and an extension of up to seven resonators [13,14]. Two nanomechanical oscillators with mechanical separation were synchronized by a photonic resonator [15] and the long-distance frequency locking between two OMOs, based on a master–slave configuration, was carried out [16]. The frequency locking of three long-distance OMOs, with the cascaded configuration, was also experimentally presented [17]. Using a class of air-slot photonic crystal OMOs cavities, two close mechanical modes could be locked [18]. In a recent experiment, an all-optical synchronization between a microdisk and a microsphere, set5 km apart with a single coherent laser, was demonstrated [19,20]. However, the OMS based on the above synchronized schemes lacked chip-scale integration, which restricted the application of reconfigurable synchronized oscillator networks due to the large-scale size. Moreover, the optical and mechanical fields were not sufficiently overlapped, resulting in a low optomechanical

coupling rate. A more suitable chip-scale synchronization platform should be explored and improved to overcome these limitations. Optomechanical crystals (OMC) [21–23] with the properties of both photonic and phononic crystals can simultaneously confine optical and mechanical modes tightly, which could generate strong interactions between optical and mechanical modes [24–27]. In the previous work, spontaneous synchronization of the coherent mechanical motion of a pair of one-dimensional silicon optomechanical photonic crystals through an engineered mechanical link was demonstrated [28].

In this paper, a new OMS consisting of parallel suspended 1D-OMC nanobeam cavities with individual optical and mechanical modes was proposed for optomechanical synchronization. The 1D-OMC nanobeam cavities were spaced apart by an air-slot gap and optically coupled by a common optical radiation field. A theoretical model was built to simulate the optomechanical synchronization. The numerical results showed that the synchronization of two mechanical breathing modes at 5.8846 GHz was achieved by using a single laser source. Such a chip-based structure has good prospects in large-scale synchronized oscillator networks, etc.

2. Theoretical Model

The individual nanobeam cavity used here had two types of periodic structures that could localize the optical and mechanical modes separately, as shown in Figure 1. The parallel OMS with the centrosymmetric structure consisted of doubly suspended nanobeams, which were spatially separated by a narrow slot gap (60–250 nm) and coupled through the optical evanescent field. The nanobeam cavities' design follows the high mechanical frequency recipe [24]. Considering the error in the manufacturing process, the geometric shape of nanobeam 2 was slightly different to that of nanobeam 1. The thickness of the silicon nanobeam was 220 nm and the width (w) was 455 nm. For nanobeam 1, the radii of the holes in photonic crystal and phononic crystal (R_h and R_n) were 136 nm and 90 nm (135.86 nm and 89.9 nm for nanobeam 2), respectively. The periodicities of photonic crystal and phononic crystal (D_h and D_n) were 487 nm and 360 nm (486.5 nm and 359.6 nm for the nanobeam 2), respectively. The radii of holes (R_1–R_4) and the corresponding periodicities (D_1–D_4) increased linearly from 99 nm to 127 nm and from 368 nm to 458 nm (from 98.9 nm to 126.87 nm and from 367.6 nm to 457.5 nm for the nanobeam 2), respectively. Each cavity of the structure supported a high-quality mechanical breathing mode to provide strong optomechanical coupling. The interaction was mechanically isolated between two 1D-OMC nanobeam cavities with a single laser driven via an efficient lensed fiber due to the air-slot gap. In the model, the mechanical coupling through the substrate connection was insignificant, as both sides had phononic crystal to protect the mechanical mode. Therefore, the two OMOs were only optically coupled through the optical evanescent field. The mechanical displacement of one OMO could generate a force to the other OMO through optical coupling, so the effective mechanical coupling was realized by both optomechanical interaction and optical coupling.

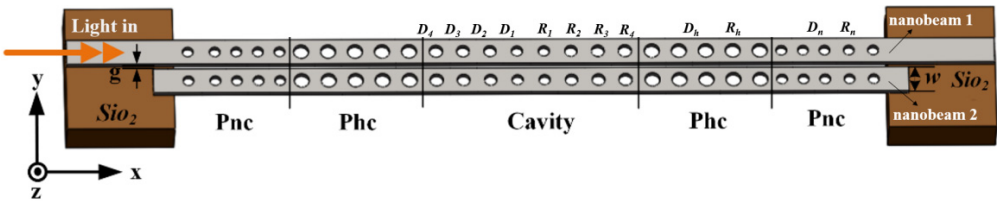

Figure 1. Schematic of the parallel OMS with doubly suspended nanobeams. Phc: photonic crystal; Pnc: phononic crystal; g: gap between nanobeam 1 and nanobeam 2; w: width of the two nanobeams.

The optical modes a_1 and a_2 of individual 1D-OMC nanobeam cavities are coupled by the near-field effect, and the coupled-mode equations are given by [8]:

$$\dot{a}_1 = \left(-\frac{\gamma_1}{2} - i\omega_1\right)a_1 + \frac{i\kappa}{2}a_2 + \sqrt{\gamma_e}a_{\text{in}}(t) \quad (1)$$

$$\dot{a}_2 = \left(-\frac{\gamma_2}{2} - i\omega_2\right)a_2 + \frac{i\kappa}{2}a_1 \quad (2)$$

where γ_i is the intrinsic loss of each cavity, the subscript i denotes 1 or 2, $\kappa/2$ is the optical coupling rate between two nanobeam cavities, γ_e is the coupling rate between the cavity and the lensed fiber, and $a_{\text{in}}(t)$ is the input optical amplitude from the lensed fiber. ω_i is the optical resonance angular frequency modulated by the mechanical displacement, which is expressed as:

$$\omega_i = \omega_{i0} + g_{om}x_i \quad (3)$$

where the g_{om} is the optomechanical coupling rate, defined as $g_{om} = \partial\omega/\partial x$, and x is the mechanical mode amplitude.

The mechanical displacements x_1 and x_2 in each cavity follow the usual optomechanical equations [8]:

$$\ddot{x}_1 = -\Gamma_1\dot{x}_1 - \Omega_1^2 x_1 + \frac{g_{om}}{m_1}\left|a_1^2\right| \quad (4)$$

$$\ddot{x}_2 = -\Gamma_2\dot{x}_2 - \Omega_2^2 x_2 + \frac{g_{om}}{m_2}\left|a_2^2\right| \quad (5)$$

where Ω_i, Γ_i, and m_i represent the mechanical resonant frequency, dissipation rate, and effective motional mass. The frequencies of optical modes a_i depend on displacements x_i. When x_1 and x_2 oscillate with frequency Ω_1 and Ω_2 near their equilibrium position, the optical force contains both the DC term and the AC term. The DC term can shift the equilibrium position of two mechanical modes. The AC term can be decomposed into harmonic forces with frequency of $p\Omega_1 + q\Omega_2$, where p and q are integers. The higher-order terms are neglected, and only the force with frequency of Ω_i is retained if $x_i \ll \Omega_i/g_{om}$. This kind of force reduces the damping rates Γ_i and leads to the coupling between x_1 and x_2. The amplitude x_1 will be much bigger than x_2, and the frequency Ω_1 is the main component in the optical force when the input power P_{in} is enough for one of the modes (for example x_1) to achieve self-sustaining optomechanical oscillation. Driven by the force with the frequency Ω_1, x_2 can oscillate with the same frequency and a smaller amplitude in comparison with x_1.

3. Results and Discussion

The transverse-electric optical modes of the two 1D-OMC nanobeam cavities were strongly coupled and split into even and odd modes, as shown in Figure 2a. The even mode had a peak electric field intensity in the center of the slot gap (see the dotted box), while there was a noticeably reduced electric field intensity in the center of the slot of the odd mode. Figure 2b shows the localized mechanical breathing mode and a corresponding mechanical frequency of 5.8877 GHz. The coupled 1D-OMC nanobeam cavities showed greater flexibility when designing the more desirable optical and mechanical modes due to having two independent nanobeam cavities and varied combinations within the architecture. The impact of the gap length on the optical modes when designing a cavity was discussed and shown in Figure 2c. The optical resonant wavelengths of the first-order optical modes based on the cavity configuration could be effectively adjusted by tuning the gap. It can be seen that the resonant wavelength of the even mode decreased with the gap, while the odd mode slowly increased with the gap. The variation trend in the wavelength could be attributed to the moving boundary effect [29]. The dominant electric field E_y was focused into the gap of the even mode, while the odd mode is the opposite. Similarly, the shift of the resonant wavelength was large with the same amount of gap variation for the even mode, in the case of a small gap. This is because the electric field in the middle of the gap was stronger.

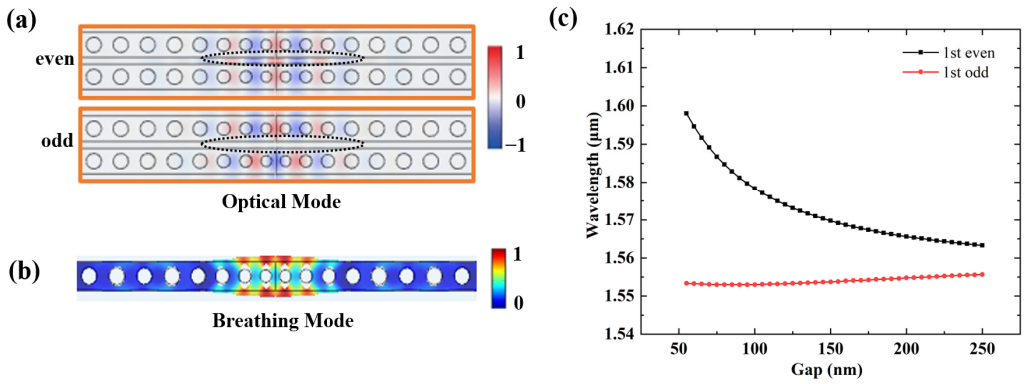

Figure 2. (**a**) Normalized electric-field amplitude E_y of even and odd optical modes; (**b**) Normalized displacement-field amplitude of the localized mechanical breathing mode in an optomechanical crystal; (**c**) Optical resonant wavelengths of odd and even modes versus gap width.

High optical quality factor Q, with a long photon lifetime in the cavity, can enhance one of the photon–phonon couplings to improve the controllability of mechanical modes. Figure 3a shows that the optical quality factor Q varied with the gap between two 1D-OMC nanobeam cavities. It should be noted that the resonant wavelength of the optical mode around 1590 nm was used as an example. The optical quality factor Q of even and odd modes were both over 10^5 at the gap range of 50–250 nm. The Q factor of the odd mode decreased with the gap, whereas the even mode had an increasing step. This was mainly due to the rapid change in the optomechanical coupling between two 1D-OMC nanobeam cavities. The optomechanical coupling rate g_{om} can characterize the interaction strength between optical and mechanical modes, which was defined as the resonant frequency shift of the optical mode caused by the mechanical motion in a 1D-OMC. The optomechanical coupling rate g_{om} calculated by the photoelastic effect and the moving boundary effect was shown in Figure 3b. It should be noted that the properties of optical and mechanical modes, including resonance frequency, Q-factor, and optomechanical coupling rate, were calculated using the finite element method (Figures 2 and 3).

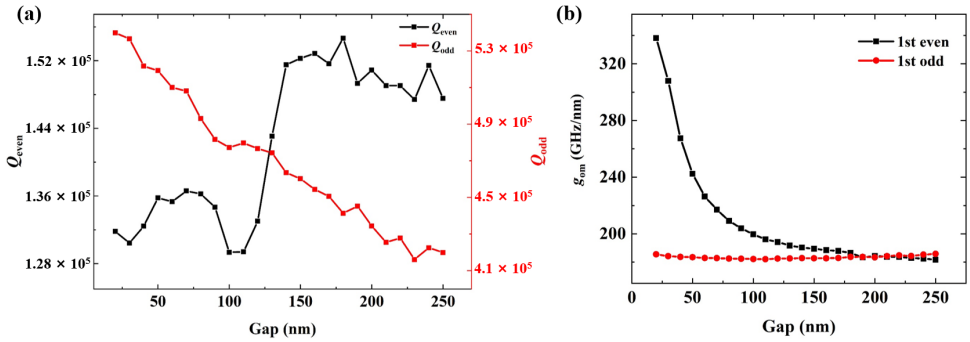

Figure 3. (**a**) Optical quality factor versus gap width; (**b**) Optomechanical coupling rate g_{om} of even and odd modes versus gap width.

When the pump laser was switched off, the mechanical displacement of the oscillator followed the usual motion equation [8]. As shown in Figure 4a, the oscillation of the top 1D-OMC nanobeam cavity experienced a rapid exponential decay during the whole time period. The mechanical frequency of the mechanical vibration was 5.8877 GHz with a high mechanical Q-factor of 2.43×10^4, as shown in Figure 4c. It is noted that the energy of the optical mode was a stable constant when there was no optomechanical coupling between optical and mechanical modes, as shown in Figure 4b.

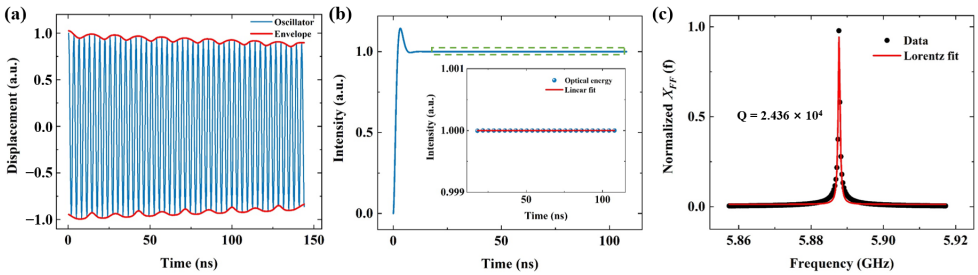

Figure 4. (**a**) Numerical solution of the motion equation; (**b**) Normalized energy of the optical mode versus the oscillate time when there is no optomechanical coupling between optical and mechanical modes; (**c**) Normalized frequency spectra of the mechanical mode in the top 1D-OMC nanobeam cavity. The inset is a detailed description of the dashed box with green.

As shown in Figure 5, a 1550 nm tunable laser was used to efficiently excite optical mode of the 1D-OMC nanobeam cavity and the strong optomechanical coupling between optical and mechanical modes was achieved. The detuning of the laser was $\Delta/\gamma = 0.25$, and the power of the laser was 300 μW. The optical force could amplify the mechanical motion via the dynamic backaction, since the blue detuning laser was used. Above a certain laser power threshold, the optomechanical amplification could overcome the mechanical damping and the OMO evolved into self-sustained oscillation, as shown in Figure 5a. Figures 4a and 5a show two different oscillating behaviors due to the optomechanical coupling between the two 1D-OMC nanobeam cavities. One is obviously attenuated, while the other oscillated steadily. Second, there was a slight difference in the frequency of the mechanical oscillator due to the optical spring effect. At the same time, the energy of the optical mode was modulated by the self-sustained oscillation of OMO and shown in Figure 5b. Figure 5c shows the frequencies of the mechanical mode and the optical force, which was consistent as well.

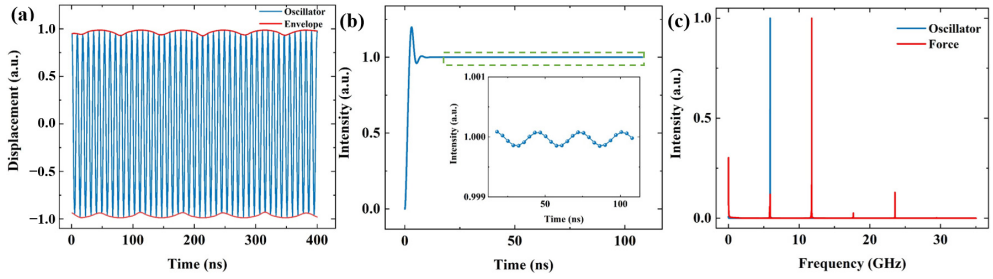

Figure 5. (**a**) Numerical solutions for the motion equation with laser excitation; (**b**) Normalized energy of the optical time versus the oscillate time, and the inset is a detailed description of the dashed box with green; (**c**) Normalized frequency spectra of the mechanical mode in the top 1D-OMC nanobeam cavity and the optical force.

The synchronization of the coupled 1D-OMC nanobeam cavities in the frequency domain is illustrated in Figure 6. Due to the slight difference in the geometry, the mechanical natural frequencies of the nanobeam cavities were 5.8877 GHz (top) and 5.9503 GHz (bottom). As shown in Figure 6a, the coupled 1D-OMC nanobeam cavities evolved to mechanical synchronization, which could be clarified in three stages. The first step was (i) the blue-shift state (0–300 μW). When the power of the pump laser increased from 0 to 300 μW, the mechanical mode appeared in the blue-shift state and gained amplitude due to the optical spring effect. The second step was (ii) the self-sustaining state (300–400 μW). Above a certain laser power, the intrinsic mechanical losses were suppressed by optomechanical amplification. The two OMOs entered self-sustained oscillation with a suddenly increased oscillation amplitude. The third step was (iii) the synchronized state (>400 μW). The two OMOs directly converted to synchronized oscillation with the same frequency.

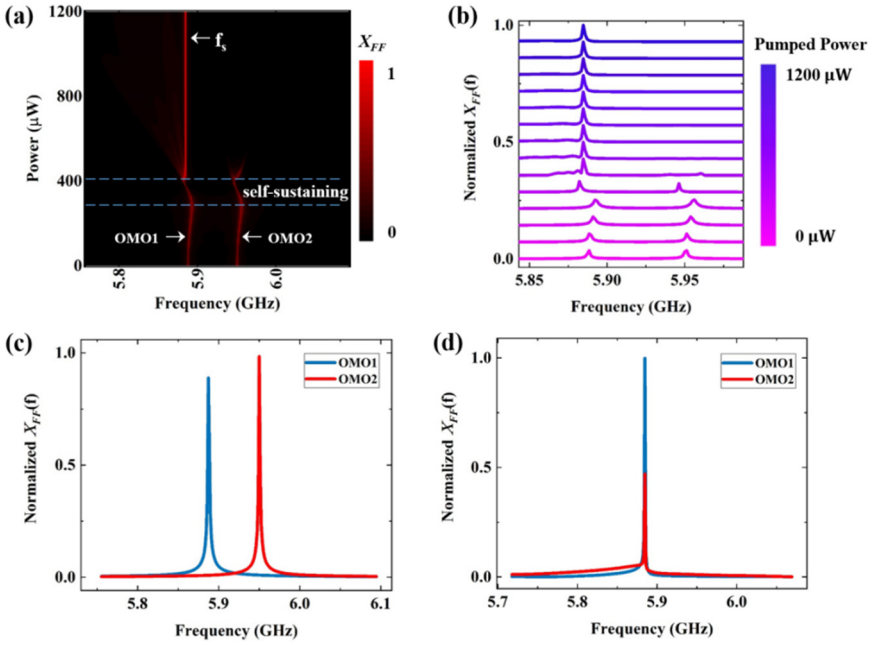

Figure 6. Synchronization of the 1D-OMC nanobeam cavities in frequency domain. (**a**) Color contour plot of the frequency spectra versus the input laser power; (**b**) Normalized frequency spectra evolution of the coupled 1D-OMC nanobeam cavities; (**c**) The frequency spectra of cavities in the unsynchronized state; (**d**) The frequency spectra of cavities in the synchronized state.

Figure 6b shows the evolution of mechanical frequency spectra when the pump laser power gradually increased. The mechanical mode experienced linewidth narrowing and oscillation amplitude gain during the three stages. Figure 6c,d show the normalized mechanical frequency modes of two OMOs with unsynchronized and synchronized states, where the blue (red) curve was the top (bottom) OMO. It is clear that the frequencies of the two OMOs were locked to 5.8846 GHz. These results confirmed that the synchronization of two mechanical breathing modes was achieved by using a single laser source. Finally, we investigated the relationship between the threshold power and the detuning of the input laser during the synchronized process. As shown in Figure 7a,b, the coupled 1D-OMC nanobeam cavities went through blue-shift and self-sustaining states and then entered the synchronized state at the detuning of 0.01 and 0.75. It could be visually resolved that the higher laser power was required at the condition of the large detuning due to the lower coupling efficiency between the input laser and the optical mode. Figure 7c shows the relationship between the threshold power (synchronization and self-sustaining) and the detuning of the input laser. The results were in good agreement with the theoretical analysis. It should be noted that the mechanical oscillating and synchronization of two 1D-OMC nanobeam cavities were achieved by using the NDSolve function in the commercial software Mathematica (Figures 4–7). The simulation method can also be extended into multiple 1D-OMC nanobeam cavities for synchronized calculation.

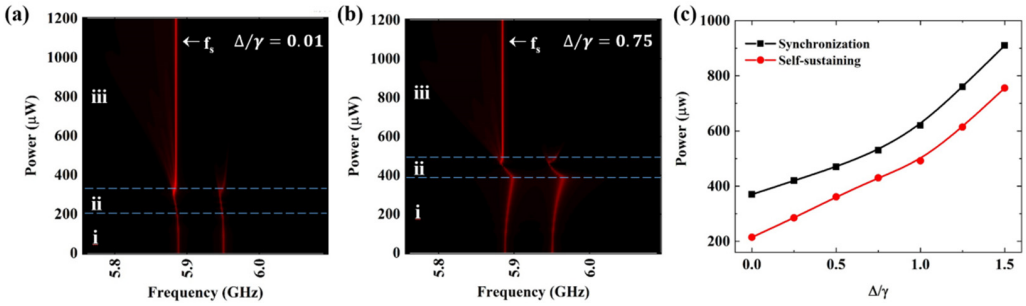

Figure 7. (**a**) Color contour plot of the frequency spectra of the coupled 1D-OMC nanobeam cavities with detuning $\Delta/\gamma = 0.01$; (**b**) Color contour plot of the frequency spectra of the coupled 1D-OMC nanobeam cavities with detuning $\Delta/\gamma = 0.75$; (**c**) The threshold power of synchronization (self-sustaining) as a function of the detuning between the optical mode and the input laser. i, ii and iii represent three stages (blue-shift state, self-sustaining state and synchronized state).

4. Conclusions

We demonstrated a new OMS consisting of parallel suspended 1D-OMC nanobeam cavities with individual optical and mechanical modes for optomechanical synchronization. Through numerical simulation, the synchronization of two mechanical breathing modes (GHz) was achieved by using a single laser source. Moreover, the configuration can be extended into multiple 1D-OMC nanobeam cavities, which indicates such a chip-based structure holds great potential toward to large-scale synchronized oscillator networks.

Author Contributions: Y.L. wrote the manuscript; F.G. performed the theoretical analysis; D.Y. presented the idea; A.W. conceived the manuscript; M.Z., S.L. and L.G. were responsible for editing; Z.Z. supervised the manuscript. All authors have read and agreed to the published version of the manuscript.

Funding: This research was funded by the National Natural Science Foundation of China (Grant No. 62105341, Grant No. 12074350), the Natural Science Foundation of Shandong Province (Grant No. ZR2021QF126), and the Science and Technology on Solid-State Laser Laboratory stability support project.

Institutional Review Board Statement: Not applicable.

Informed Consent Statement: Not applicable.

Data Availability Statement: Not applicable.

Conflicts of Interest: The authors declare no conflict of interest.

References

1. Sivrikaya, F.; Yener, B. Time synchronization in sensor networks: A survey. *IEEE Network* **2004**, *18*, 45–50. [CrossRef]
2. Shanmugam, L.; Mani, P.; Rajan, R.; Joo, Y.H. Adaptive synchronization of reaction–diffusion neural networks and its application to secure communication. *IEEE Trans. Cybernetics* **2018**, *50*, 911–922. [CrossRef] [PubMed]
3. Mahboob, I.; Yamaguchi, H. Bit storage and bit flip operations in an electromechanical oscillator. *Nat. Nanotechnol.* **2008**, *3*, 275–279. [CrossRef] [PubMed]
4. Bagheri, M.; Poot, M.; Li, M.; Pernice, W.P.H.; Tang, H.X. Dynamic manipulation of nanomechanical resonators in the high-amplitude regime and non-volatile mechanical memory operation. *Nat. Nanotechnol.* **2011**, *6*, 726–732. [CrossRef]
5. Shim, S.B.; Imboden, M.; Mohanty, P. Synchronized oscillation in coupled nanomechanical oscillators. *Science* **2007**, *316*, 95–99. [CrossRef]
6. Matheny, M.H.; Grau, M.; Villanueva, L.G.; Karabalin, R.B.; Cross, M.C.; Roukes, M.L. Phase Synchronization of Two Anharmonic Nanomechanical Oscillators. *Phys. Rev. Lett.* **2014**, *112*, 014101. [CrossRef]
7. Agrawal, D.K.; Woodhouse, J.; Seshia, A.A. Observation of locked phase dynamics and enhanced frequency stability in synchronized micromechanical oscillators. *Phys. Rev. Lett.* **2013**, *111*, 084101. [CrossRef]
8. Aspelmeyer, M.; Kippenberg, T.J.; Marquardt, F. Cavity optomechanics. *Rev. Mod. Phys.* **2014**, *86*, 1391. [CrossRef]
9. Kippenberg, T.J.; Vahala, K.J. Cavity opto-mechanics. *Opt. Express* **2007**, *15*, 17172–17205. [CrossRef]
10. Heinrich, G.; Ludwig, M.; Qian, J.; Kubala, B.; Marquardt, F. Collective dynamics in optomechanical arrays. *Phys. Rev. Lett.* **2011**, *107*, 043603. [CrossRef]

11. Shlomi, K.; Yuvaraj, D.; Baskin, I.; Suchoi, O.; Winik, R.; Buks, E. Synchronization in an optomechanical cavity. *Phys. Rev. E* **2015**, *91*, 032910. [CrossRef] [PubMed]
12. Holmes, C.A.; Meaney, C.P.; Milburn, G.J. Synchronization of many nanomechanical resonators coupled via a common cavity field. *Phys. Rev. E* **2012**, *85*, 066203. [CrossRef] [PubMed]
13. Zhang, M.; Wiederhecker, G.S.; Manipatruni, S.; Barnard, A.; McEuen, P.; Lipson, M. Synchronization of micromechanical oscillators using light. *Phys. Rev. Lett.* **2012**, *109*, 233906. [CrossRef] [PubMed]
14. Zhang, M.; Shah, S.; Cardenas, J.; Lipson, M. Synchronization and phase noise reduction in micromechanical oscillator arrays coupled through light. *Phys. Rev. Lett.* **2015**, *115*, 163902. [CrossRef]
15. Bagheri, M.; Poot, M.; Fan, L.; Marquardt, F.; Tang, H.X. Photonic cavity synchronization of nanomechanical oscillators. *Phys. Rev. Lett.* **2013**, *111*, 213902. [CrossRef]
16. Shah, S.Y.; Zhang, M.; Rand, R.; Lipson, M. Master-slave locking of optomechanical oscillators over a long distance. *Phys. Rev. Lett.* **2015**, *114*, 113602. [CrossRef]
17. Gil-Santos, E.; Labousse, M.; Baker, C.; Goetschy, A.; Hease, W.; Gomez, C.; Lemaître, A.; Leo, G.; Ciuti, C.; Favero, I. Light-mediated cascaded locking of multiple nano-optomechanical oscillators. *Phys. Rev. Lett.* **2017**, *118*, 063605. [CrossRef]
18. Huang, Y.; Wu, J.; Flores, J.G.F.; Yu, M.; Kwong, D.L.; Wen, G.; Wong, C.W. Synchronization in air-slot photonic crystal optomechanical oscillators. *Appl. Phys. Lett.* **2017**, *110*, 111107. [CrossRef]
19. Li, T.; Bao, T.Y.; Zhang, Y.L.; Zou, C.L.; Zou, X.B.; Guo, G.C. Long-distance synchronization of unidirectionally cascaded optomechanical systems. *Opt. Express* **2016**, *24*, 12336–12348. [CrossRef]
20. Li, J.; Zhou, Z.H.; Wan, S.; Zhang, Y.L.; Shen, Z.; Li, M.; Zou, C.L.; Guo, G.C.; Dong, C.H. All-optical synchronization of remote optomechanical systems. *Phys. Rev. Lett.* **2022**, *129*, 063605. [CrossRef]
21. Chan, J.; Eichenfield, M.; Camacho, R.; Painter, O. Optical and mechanical design of a "zipper" photonic crystal optomechanical cavity. *Opt. Express* **2009**, *17*, 3802–3817. [CrossRef] [PubMed]
22. Quan, Q.; Loncar, M. Deterministic design of wavelength scale, ultra-high Q photonic crystal nanobeam cavities. *Opt. Express* **2011**, *19*, 18529–18542. [CrossRef] [PubMed]
23. Eichenfield, M.; Chan, J.; Camacho, R.M.; Vahala, K.J.; Painter, O. Optomechanical crystals. *Nature* **2009**, *462*, 78–82. [CrossRef] [PubMed]
24. Huang, Z.; Cui, K.; Li, Y.; Feng, X.; Liu, F.; Zhang, W.; Huang, Y. Strong optomechanical coupling in nanobeam cavities based on hetero optomechanical crystals. *Sci. Rep.* **2015**, *5*, 15964. [CrossRef] [PubMed]
25. Li, Y.; Cui, K.; Feng, X.; Huang, Y.; Huang, Z.; Liu, F.; Zhang, W. Optomechanical Crystal Nanobeam Cavity with High Optomechanical Coupling Rate. *J. Opt.* **2015**, *17*, 045001. [CrossRef]
26. Wu, N.; Cui, K.Y.; Feng, X.; Liu, F.; Zhang, W.; Huang, Y.D. Hetero-Optomechanical Crystal Zipper Cavity for Multimode Optomechanics. *Photonics* **2022**, *9*, 78. [CrossRef]
27. Xu, Q.C.; Cui, K.Y.; Wu, N.; Feng, X.; Liu, F.; Zhang, W.; Huang, Y.D. Tunable mechanical-mode coupling based on nanobeam-double optomechanical cavities. *Photonics Res.* **2022**, *10*, 1819–1827. [CrossRef]
28. Colombano, M.F.; Arregui, G.; Capuj, N.E.; Pitanti, A.; Maire, J.; Griol, A.; Garrido, B.; Martinez, A.; SotomayorTorres, C.M.; Navarro-Urrios, D. Synchronization of Optomechanical Nanobeams by Mechanical Interaction. *Phys. Rev. Lett.* **2019**, *123*, 017402. [CrossRef]
29. Safavi-Naeini, A.H.; Van Thourhout, D.; Baets, R.; Van Laer, R. Controlling Phonons and Photons at the Wavelength-Scale: Silicon Photonics Meets Silicon Phononics. *Optica* **2019**, *6*, 213. [CrossRef]